Electric Power Systems Research 196 (2021) 107273

Contents lists available at ScienceDirect

Electric Power Systems Research

journal homepage: www.elsevier.com/locate/epsr

Stabilization of MT-HVDC grids via passivity-based control and convex optimization

Oscar Danilo Montoya [a,b], Walter Gil-González [c], Alejandro Garces [d], Federico Serra [e], Jesus C. Hernández [*,f]

[a] Facultad de Ingeniería, Universidad Distrital Francisco José de Caldas. Carrera 7 No. 40B - 53, Bogotá D.C 11021, Colombia
[b] Laboratorio Inteligente de Energía, Universidad Tecnológica de Bolívar, Cartagena 131001, Colombia
[c] Facultad de Ingeniería, Institución Universitaria Pascual Bravo, Campus Robledo, Medellín 050036, Colombia
[d] Programa de Ingeniería Eléctrica, Universidad Tecnológica de Pereira. AA: 97 - Postcode: Pereira 660003, Colombia
[e] Laboratorio de Control Automático (LCA), Facultad de Ingeniería y Ciencias Agropecuarias, Universidad Nacional de San Luis, Villa Mercedes, 5730, Argentina
[f] Department of Electrical Engineering, University of Jaén, Campus Lagunillas s/n, Edificio A3, Jaén 23071, Spain

ARTICLE INFO

Keywords:
Convex optimization
Direct-current networks
Passivity-based control
Hierarchical control
Port-Hamiltonian formulation
Stabilization of electrical networks

ABSTRACT

This paper presents a model for stabilizing multi-terminal high voltage direct-current (MT-HVDC) networks with constant power terminals (CPTs) interfaced with power electronic converters. A hierarchical structure of hierarchical control is developed, which guarantees a stable operation under load variations. This structure includes a port-Hamiltonian formulation representing the network dynamics and a passivity-based control (PBC) for the primary control. This control guarantees stability according to Lyapunov's theory. Next, a convex optimal power flow formulation based on semidefinite programming (SDP) defines the control's set point in the secondary/tertiary control. The proposed stabilization scheme is general for both point-to-point HVDC systems and MT-HVDC grids. Simulation results in MATLAB/Simulink demonstrate the stability of the primary control and the optimal performance of the secondary/tertiary control, considering three simulation scenarios on a reduced version of the CIGRE MT-HVDC test system: (i) variation of generation and load, (ii) short-circuit events with different fault resistances and (iii) grid topology variation. These simulations prove the applicability and efficiency of the proposed approach.

1. Introduction

Renewable sources and energy storage devices are integrated using power electronic converters, which allow the use of multi-terminal high voltage direct current MT-HVDC networks. These technologies allow to obtain advantages, such as lower losses, lack of synchronization, reactive power requirements, and high-reliability [1]. These networks require to act coordinately in order to guarantee stability and optimal operation. Renewable sources need to be operated coordinately to preserve suitable nodal voltage and maintain the energy storage devices between their operation limits. The grid must also preserve a constant power consumption at specific points named as constant power terminals (CPTs) [2,3].

The operation of MT-HVDC networks requires integrating advanced control and optimization techniques. The former is required to operate power electronic converters associated with each energy resource [4,5] and the latter is required to define the best operation point [6,7]. Hence, a primary control stabilizes the network in a particular operating point, and a secondary/tertiary control defines the best operative point considering economic and physical constraints [6,8].

The control of an MT-HVDC is similar to a stand-alone DC microgrid which includes a hierarchical control. In [9], a port-Hamiltonian model in conjunction with the interconnection and damping assignment passivity-based control (PBC) was presented for the primary control. In [8], an optimal power flow from a dynamic analysis based on port-Hamiltonian models for controlling power flows in MT-HVDC systems was proposed. This same approach was adopted in [10] via port-Hamiltonian models for resistive networks. The authors in [11,12] proposed consensus strategies for power-sharing in DC networks with multiple constant power loads and distributed energy resources. While

* Corresponding author.
E-mail addresses: odmontoyag@udistrital.edu.co (O.D. Montoya), walter.gil@pascualbravo.edu.co (W. Gil-González), alejandro.garces@utp.edu.co (A. Garces), serrafederico@gmail.com (F. Serra), jcasa@ujaen.es (J.C. Hernández).

https://doi.org/10.1016/j.epsr.2021.107273
Received 29 December 2020; Received in revised form 31 March 2021; Accepted 10 April 2021
Available online 30 April 2021

in [13], the authors combined the consensus algorithm to a plug-and-play control approach for power control in DC networks. The authors in [14] presented a detailed revision of different control architectures for the voltage and power regulation of DC networks via a hierarchical control. Some distributed control approaches were also discussed in [15,16] considering grid topology variations or communication delays. The authors in [4] proposed a general nonlinear control with feedback based on the Lyapunov control theory to stabilize DC networks with multiple CPTs and actuators for islanded grid applications by modeling each power electronic converter. In [17], a predictive fuzzy control model for the dynamic stabilization of DC microgrids is proposed. In [18], a nonlinear stabilization method for DC networks using a curvature Kalman filter was recently proposed.

In the secondary/tertiary control, most of the publications reported in the specialized literature focus on an optimal power flow (OPF) solution via metaheuristic or exact mathematical techniques [19]. The authors in [7] presented a hybrid Gauss-Seidel genetic algorithm for solving the OPF problem in DC networks with multiple CPTs and voltage-controlled nodes. The authors in [2] provided a convex optimization model based on second-order cone programming for solving the OPF problem in islanded DC networks with CPTs. In contrast, [20] proposed semidefinite programming (SDP) model for determining the voltage stability index on DC networks via OPF formulation. The authors in [21] presented a multi-period SDP model for the economic dispatch of renewable generation and batteries in DC networks. The authors in [22] proposed an SDP model for an OPF solution in high-voltage DC networks by including a quadratic formulation of the power losses in the DC-DC converters. Whereas [6] proposed a convex model for solving the OPF problem via Taylor's series approximation of the power balance equations.

Based on the review mentioned in the above state-of-the-art, we propose a combination of the PBC theory for primary (stabilization) control purposes on DC networks. This method guarantees globally asymptotic stability properties. In comparison with the recent contribution presented in [9], the main advantage of this approach is that our proposed PBC control does not require communication channels in the control step and avoids parametric dependence on the capacitive filter values at each power electronic converter. The approach in [9] required this information to develop its PBC control strategy. Additionally, to define the desired operative point for the proposed PBC approach, we proposed as a secondary/tertiary control approach an OPF methodology based on an SDP model. This optimization strategy guarantees uniqueness in the solution as presented in [21]. This hierarchical control exploits the most important advantages of nonlinear control and convex optimization to propose a robust DC grid operation strategy that was not previously found in the specialized literature. According to the above, the contributions of this study can be summarized:

- A primary control for MT-HVDC grids with CPTs based on passivity theory is described. The proposed strategy uses a PI control to stabilize the DC-voltage and guarantee stability using Lyapunov's theory.
- A secondary/tertiary control based on the SDP model for minimizing the power losses in MT-HVDC grid is developed.
- The proposed control's performance is analyzed for the different values of proportional and integral gains. Furthermore, the robustness is also investigated under large disturbances as faults and tripping transmission lines.

The rest of the paper is organized as follows: Section 2 presents the mathematical modeling of MT-HVDC and its dynamic representation for primary control purposes and its static formulation for secondary/tertiary control. Section 3 presents the PBC theory's mathematical foundation for nonlinear port-Hamiltonian systems and the different control designs, including the proportional and PI PBC proposed approaches. Section 4 shows the desired operative point's selection via convex optimization by showing the original non-convex OPF model's transformation into a convex representation via an SDP relaxation. In Section 5, a pseudo-code compacts the proposed hierarchical control methodology. In contrast, Section 6 presents the simulation results in MATLAB/Simulink that demonstrate the stability of the primary control and the optimal performance of the secondary/tertiary control, considering three simulation scenarios on a reduced version of the CIGRE MT-HVDC test system. Finally, in Section 7, the main conclusions derived from this work are presented.

2. Network modeling

An MT-HVDC may contain different active components as depicted in Fig. 1. Its mathematical representation depends on whether the objective is to stabilize or optimize the operation. While a dynamic model is essential in the former case, a steady-state model is sufficient in the latter situation [6]. Both models are nonlinear and highly interconnected, so it is a challenge for theoretical and practical viewpoints. Thus, a dynamic model from an MT-HVDC network requires focusing on the power electronic converters [9]. In contrast, an optimization model needs a detailed representation of the network configuration, but a simplified description of those converters [23,24]. Fig. 2 illustrates the control structure of a conventional DC-bus voltage, which is composed of an inner loop (current control) and an outer loop (voltage control) [25].

In addition to renewable generation sources, an MT-HVDC grid may include CPTs. These terminals introduce a negative resistive effect that reduces the stability margin of the system. Besides, they add nonlinear and non-convex constraints into optimization models, so they are also a challenge for the secondary/tertiary control. These aspects are discussed below.

2.1. Dynamic modeling

A CPT is usually interconnected to a power electronic converter. However, it is convenient to simplify its model as presented in Fig. 3.

By applying Kirchhoff's first law at node k, the following first-order differential equation is obtained:

$$c_k \dot{v}_k = p_k v_k^{-1} - g_k v_k - i_k, \tag{1}$$

where c_k corresponds to the capacitive shunt filter associated with the power electronic converter connected at node k; g_k represents a linear

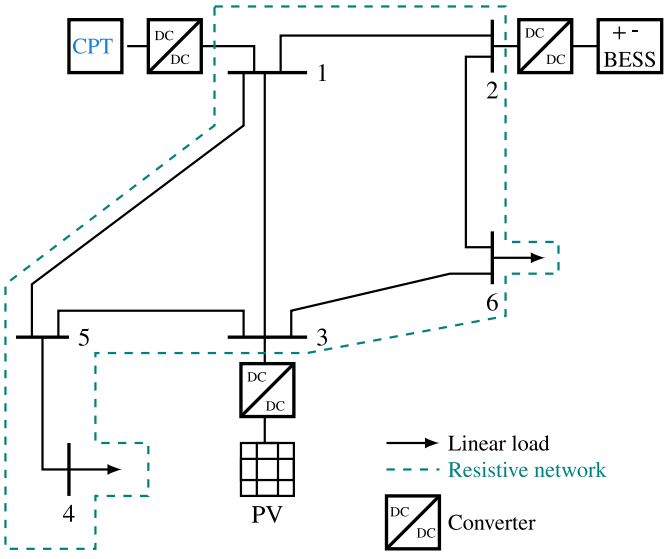

Fig. 1. Schematic representation of a MT-HVDC network with energy resources, storage, linear loads, and constant power loads.

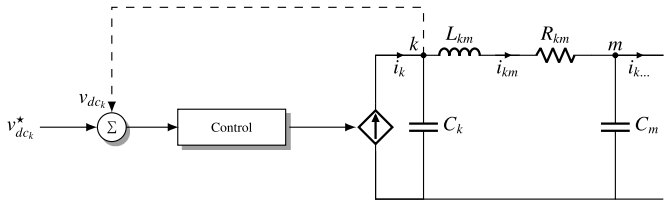

Fig. 2. Block diagram of a conventional control for the DC-bus voltage controlled.

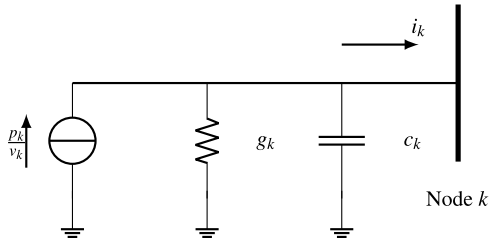

Fig. 3. Simplified model of a constant power terminal [9].

resistive load connected at node k; p_k is the constant power value managed by the power electronic converter, which is positive for generators and negative for CPTs; i_k is the total injected current at node k; and v_k represents its voltage.

For compactness purposes on the dynamic modeling given by Eq. (1), all power electronic converter nodes were grouped in the set $\mathscr{S}$ with cardinality s, which implies that Eq. (1) can be rewritten with a matrix form as presented below:

$$C_{\mathscr{S}}\dot{v}_{\mathscr{S}} = \text{diag}\left(v_{\mathscr{S}}^{-1}\right)p_{\mathscr{S}} - G_{\mathscr{S}}v_{\mathscr{S}} - i_{\mathscr{S}}, \tag{2}$$

where $C_{\mathscr{S}} \in \mathbb{R}^{s\times s}$ is a positive definite matrix that contains all the capacitive effects of the power electronic converter; $G_{\mathscr{S}} \in \mathbb{R}^{s\times s}$ is a positive semidefinite matrix that contains all the conductive effects at the nodes contained in the set $\mathscr{S}$; $\text{diag}^{-1}(v_{\mathscr{S}}) \in \mathbb{R}^{s\times s}$ corresponds to a positive definite matrix with the inverse of each voltage at its diagonal; $i_{\mathscr{S}} \in \mathbb{R}^{s\times 1}$ represents the vector of injected currents while $v_{\mathscr{S}} \in \mathbb{R}^{s\times 1}$ corresponds to the voltage at the power electronic converter.

Now, we focus on the MT-HVDC network that interconnects the power electronic converters to the other nodes (see Fig. 1). This grid can be modeled by an admittance matrix that represents the nodal relation between net injected currents and voltage nodes. We apply the voltage nodal method as presented below:

$$\begin{pmatrix} i_{\mathscr{S}} \\ i_{\mathscr{R}} \end{pmatrix} = \begin{bmatrix} G_{\mathscr{S}\mathscr{S}} & G_{\mathscr{S}\mathscr{R}} \\ G_{\mathscr{R}\mathscr{S}} & G_{\mathscr{R}\mathscr{R}} \end{bmatrix} \begin{pmatrix} v_{\mathscr{S}} \\ v_{\mathscr{R}} \end{pmatrix}, \tag{3}$$

where $G_{\mathscr{S}\mathscr{S}} \in \mathbb{R}^{s\times s}$ represents the conductance between power electronic converters; $G_{\mathscr{S}\mathscr{R}} \in \mathbb{R}^{s\times r}$ and $G_{\mathscr{R}\mathscr{S}} \in \mathbb{R}^{r\times s}$ define the admittance between power electronic converters and linear nodes[1]; whereas $G_{\mathscr{R}\mathscr{R}} \in \mathbb{R}^{r\times r}$ determines the conductance between linear nodes; r corresponds to the cardinality of the set $\mathscr{R}$ associated with the linear nodes; finally $i_{\mathscr{R}} \in \mathbb{R}^{r\times 1}$ and $v_{\mathscr{R}} \in \mathbb{R}^{r\times 1}$ correspond to the injected current and nodal voltage at linear nodes.

Notice that the injected current at linear nodes is identically to zero, i.e., $i_{\mathscr{R}}$, since not constant power loads, distributed generators, energy storage systems or grid interconnections appear in these nodes (see nodes 4 and 6 in Fig. 1). Therefore, by applying the Kron's reduction over Eq. (3), the following result is reached [26]:

$$i_{\mathscr{S}} = \left(G_{\mathscr{S}\mathscr{S}} - G_{\mathscr{S}\mathscr{R}}G_{\mathscr{R}\mathscr{R}}^{-1}G_{\mathscr{R}\mathscr{S}}\right)v_{\mathscr{S}} = Y_{\mathscr{S}\mathscr{S}}v_{\mathscr{S}}, \tag{4}$$

where $Y_{\mathscr{S}\mathscr{S}} \in \mathbb{R}^{s\times s}$ represents the equivalent admittance between power-controlled nodes after applying a Kron's reduction. Note that the Kron's reduction is possible since $G_{\mathscr{R}\mathscr{R}}$ is a positive definite matrix, i.e., it has inverse.

Finally, to achieve the final dynamic modeling of the MT-HVDC network for control purposes, Eq. (4) is substituted in Eq. (2) which produces the following result:

$$C_{\mathscr{S}}\dot{v}_{\mathscr{S}} = \text{diag}^{-1}(v_{\mathscr{S}})p_{\mathscr{S}} - K_{\mathscr{S}}v_{\mathscr{S}}, \tag{5}$$

where $K_{\mathscr{S}} = G_{\mathscr{S}} + Y_{\mathscr{S}\mathscr{S}}$.

2.2. Stationary-state modeling

Conventionally, a DC grid can be modeled by a set of nonlinear non–convex equations for power flow and optimal power flow problems [2,20]. These models assume that all the voltages of the DC network have been stabilized by a primary control, which implies that the system is in a stationary state [21]. Considering this assumption, $\dot{v}_{\mathscr{S}} = 0$ and Eq. (5) can be rewritten under steady-state as follows:

$$p_{\mathscr{S}} = \text{diag}(v_{\mathscr{S}})K_{\mathscr{S}}v_{\mathscr{S}}. \tag{6}$$

Power system readers widely know expression in Eq. (6) as the set of power flow equations for DC networks with CPTs. Some recent investigations have also demonstrated that these equations can be solved by Newton–Raphson methods [3], Gauss-Seidel approximations [7,26], or linear methods [6,23]. In this paper, those equations are essential input for formulating a convex optimization problem with a unique solution to determine the set-point, as discussed in the next section.

3. Stabilization by passivity–based control

The PBC approach is a well-studied and strong mathematically founded nonlinear control technique for designing systems with Lagrangian or Hamiltonian representation. This method guarantees stability in the sense of Lyapunov's for closed-loop operation [27,28]. It exploits the strong relation between the energy storage in the system and its dynamics to generate a control strategy that preserves passive and dissipative properties [29,30]. Based on the well-known passive properties of electrical networks, we proposed a control using a port-Hamiltonian formulation [31].

Proposition 1. *The reduced dynamic system in Eq. (5) can be represented as a port-Hamiltonian system with an affine structure as follows:*

$$\mathscr{D}\dot{x} = (\mathscr{M} - \mathscr{N})x + \mathscr{G}(x)u, \tag{7}$$

where $\mathscr{D} \in \mathbb{R}^{s\times s}$ is a positive definite matrix known as the inertia matrix; $\mathscr{M} \in \mathbb{R}^{s\times s}$ and $\mathscr{N} \in \mathbb{R}^{s\times s}$ correspond to the interconnection and damping matrix, which are skew–symmetric and positive semidefinite, respectively; $x \in \mathbb{R}^{s\times 1}$ represents the vector of the state variables, $\mathscr{G}(x) \in \mathbb{R}^{s\times s}$ corresponds to the positive define input matrix and $u \in \mathbb{R}^{s\times 1}$ is the input vector.

Proof. The proof of this proposition is straightforward by comparing Eq. (5) to Eq. (7) and making the following definitions:

$$x = v_{\mathscr{S}},\ u = p_{\mathscr{S}},\ \mathscr{D} = C_{\mathscr{S}} \tag{8}$$

$$\mathscr{M} = 0,\ \mathscr{N} = \mathscr{K}_{\mathscr{S}},\ \mathscr{G}(x) = \text{diag}^{-1}(v_{\mathscr{S}}). \tag{9}$$

□ To define a control law that allows moving the current operative point x to the desired operative point $x^{\star}$, let us define the dynamics of the error in the state variables as $\tilde{x} = x - x^{\star}$; besides, it is clear that for DC grids $x^{\star}$ is constant, which implies that $\dot{\tilde{x}} = \dot{x}$.

[1] Note that $G_{\mathscr{R}\mathscr{S}} = G_{\mathscr{S}\mathscr{R}}^{\top}$

Proposition 2. *A control input u exists such that the port-Hamiltonian system in Eq. (7) takes a gradient form for a closed-loop operation as presented below:*

$$\mathscr{D}\dot{x} = -\mathscr{N}_{\star}\tilde{x}, \tag{10}$$

where $\mathscr{N}_{\star}$ is a positive definite matrix that guarantees that (10) is exponentially stable.

Proof. To determine the control input law that allows transforming Eq. (7) into Eq. (10), both equations are equaled by assuming that $\mathscr{G}(x)$ is a full–rank square invertible matrix. This is a reasonable assumption since the voltages x must be guaranteed for DC grid operation and contained between $x_{\min}$ and $x_{\max}$, such that $x_{\min} > 0$. Considering this assumption, then the control input takes the following form, and the proof is completed:

$$u = \mathscr{G}^{-1}(x)(\mathscr{N}x - \mathscr{N}_{\star}\tilde{x}), \tag{11}$$

where $\mathscr{N}_{\star} \in \mathbb{R}^{s\times s}$ is a positive definite matrix that contains all control gains. □ The proposed control law defined by Eq. (11) was initially proposed by [9]. Nevertheless, the control law's main disadvantage is its dependence on the voltage measurements at all power electronic converter nodes since $\mathscr{N}$ corresponds to a full rank matrix.

For providing an alternative control law that avoids depending on voltage measurements at each power electronic converter, we propose a modification to Eq. (11) as follows:

$$u = \mathscr{G}^{-1}(x)(\mathscr{N}x^{\star} - \mathscr{N}_{\star}\tilde{x}). \tag{12}$$

Proposition 3. *The control law in Eq. (12) guarantees a global asymptotic stable response for the dynamic system in Eq. (7).*

Proof. To obtain a closed–loop dynamic behavior of the system in Eq. (7), let us substitute Eq. (12) with Eq. (7) and rearrange some terms as follows:

$$\mathscr{D}\dot{x} = -(\mathscr{N} + \mathscr{N}_{\star})\tilde{x}. \tag{13}$$

To proof the exponential stability of the dynamic system given by Eq. (3), let us define the following candidate Lyapunov function [28]:

$$\mathscr{V}(\tilde{x}) = \frac{1}{2}\tilde{x}^{\top}\mathscr{D}\tilde{x}. \tag{14}$$

Applying the temporal derivative of $\mathscr{V}(\tilde{x})$ and considering that $\mathscr{D} = \mathscr{D}^{\top}$, the following result is achieved:

$$\dot{\mathscr{V}}(\tilde{x}) = -\tilde{x}^{\top}(\mathscr{N} + \mathscr{N}_{\star})\tilde{x}. \tag{15}$$

The result given by Eq. (15) shows that the dynamic system in Eq. (13) is asymptotically stable according to Lyapunov's theory [31]. Furthermore, it is also exponentially stable since, $\dot{\mathscr{V}}(\tilde{x}) \leq -\beta\mathscr{V}(\tilde{x})$ if we select $\beta \leq \lambda_{\min}(\mathscr{D}^{-1}(\mathscr{N} + \mathscr{N}_{\star}))$. □

An integral action can be added to the control for reducing steady state errors without affecting the exponential stability of the closed-loop dynamic system as presented below:

$$\begin{aligned} u &= \mathscr{G}^{-1}(x)(\mathscr{N}x^{\star} - \mathscr{N}_{\star}\tilde{x} - \mathscr{K}_i z), \\ \dot{z} &= \tilde{x}, \end{aligned}$$

where $\mathscr{K}_i = \mathscr{K}_i^{\top}$ corresponds to a symmetric matrix that contains all integral gains. For proving the asymptotically stability of these PI control refer to [27].

Fig. 4 depicts the proposed control implemented at node k. Initially, the control law computed in Eq. (14) is a power. Therefore, the control law is converted into a current dividing by the dc-voltage at node k. However, the control law is also multiplied by this same dc-voltage. Hence, this step was simplified.

4. Convex OPF for reference selection

The set-points primary control set-points constitute a secondary/tertiary layer, typically associated with an optimization model. Hence, the system dynamics are usually negligible since this optimization layer focuses on obtaining the desired operative point under steady-state conditions. The static DC model presented in Eq. (6) is involved inside optimal power flow problems as a balanced power set of constraints [6]. This paper focuses on a convex transformation of the classical nonlinear non-convex OPF problem since the convex model guarantees a global optimum solution with low computational effort [22,32].

The nonlinear non-convex conventional OPF problem has the following model:

Model 1 (Non convex OPF-DC).

$$\begin{aligned} \text{Minimize} \quad & p_{\text{loss}} = x^{\top}\mathscr{Y}_{\mathscr{DD}}x \\ & p_{\mathscr{J}} = p^{g}_{\mathscr{J}} - p^{d}_{\mathscr{J}} = \text{diag}(x)\mathscr{K}_{\mathscr{J}}x \\ & p^{g,\min}_{\mathscr{J}} \leq p^{g}_{\mathscr{J}} \leq p^{\max}_{g} \\ & x_{\min} \leq x \leq x_{\max} \end{aligned} \tag{16}$$

where $p_{loss} \in \mathbb{R}^{+}$ is the objective function associated to the active power losses, $p^{g}_{\mathscr{J}} \in \mathbb{R}^{s\times s}$ and $p^{d}_{\mathscr{J}} \in \mathbb{R}^{s\times s}$ represent the power generation and load consumption at distributed energy resource nodes and CPTs, respectively.

Notice that the solution of the optimization problem given by (16) corresponds to the set-point $x^{\star}$ for the control problem treated previously. Nevertheless, the solution of **Model 1** is not easy since the power flow balance is nonlinear and non-convex. For this reason, we use the

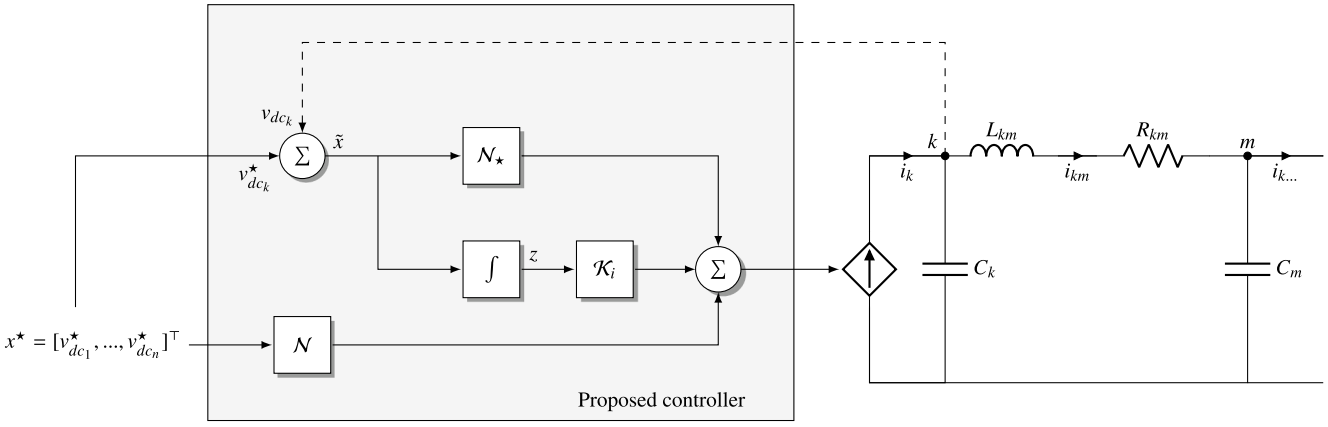

Fig. 4. Block diagram of the proposed control for voltage control

convex reformulation of the OPF problem as proposed in [21] to obtain its approximated solution to guarantee uniqueness in the solution [33].

Model 1 is reformulated as a convex problem via SDP approximation. Let us define $X = xx^{\top}$ as a decision matrix, which entails to the following transformation:

Model 2 (SDP convex OPF-DC).

$$\begin{aligned} \text{Minimize} \quad & p_{\text{loss}} = \text{tr}(X) \\ & p^{g}_{\mathscr{J}} - p^{d}_{\mathscr{J}} = \text{diag}(\mathscr{H}_{\mathscr{J}} X) \\ & p^{g,\min}_{\mathscr{J}} \leq p^{g}_{\mathscr{J}} \leq p^{\max}_{g} \\ & \mathbf{1}_{\mathscr{J}} x^{2}_{\min} \leq X \leq \mathbf{1}_{\mathscr{J}} x^{2}_{\max} \\ & X = X^{\top} \succeq 0 \end{aligned} \tag{17}$$

where $\text{tr}(\cdot)$ is the trace and $\mathbf{1}_{\mathscr{J}} \in \mathbb{R}^{s \times s}$ is a matrix filled by ones.

Notice that **Model 2** is convex since the rank matrix constrain $rank(X) = 1$ was relaxed [20].

It can be observed that the result of the SDP is a rank s matrix. Therefore, it is necessary to employ a general decomposition to recover the vector x from matrix X. To achieve this, it uses the decomposition method by means of eigenvalues and eigenvectors [21,22] as follows:

$$X = \sum_{k=1}^{s} \lambda_k W_k W_k^{\top}, \tag{18}$$

where λ_k and W_k represent eigenvalues and their corresponding eigenvectors in each time period, respectively. If the representation for the problem as an SDP is good enough, $s-1$ eigenvalues close to zero are expected. Therefore, the rank of X is an approximation to one and can be achieved as presented below:

$$X \approx \lambda_m W_m W_m^{\top}, \tag{19}$$

where λ_m represents the maximum eigenvalue (i.e other eigenvalues are close to zero) in each time period. According to this approximation, it is possible to recover the vector x as follows:

$$x \approx \sqrt{\lambda_m} W_m^{\top}, \tag{20}$$

The main advantage of this methodology is its efficiency and precision [34].

5. Hierarchical control

The pseudo-code presented in Algorithm 1 shows the coordinate control strategy for stabilizing DC networks using PBC theory in conjunction with convex optimization.

This hierarchical control scheme solves the proposed convex OPF model recursively each time the DC grid has any change to update the control input so that the DC network remains stable. Fig. 5 shows the proposed hierarchical control scheme.

6. Computational validation

To validate the proposed hierarchical control, we consider a reduced version of the CIGRE MT-HVDC system presented in [25]. It is composed of six buses and five power electronic interfaces as presented in Fig. 6. This system is operated with 400 kV, and we assume that the slack source is located at node 1. In addition, the parametric information of the overhead lines (OHL) and the cables (CBL) is listed in Table 1.

Due to the length of the HVDC transmission lines, these are represented with $\pi-$ equivalents. Table 2 lists the complete information of the lines for the HVDC system depicted in Fig. 6.

The information reported in Table 2 is used to calculate the reduced conductance matrix under steady-state conditions (i.e., eliminating nodes 6 and 7), which take the following form in per-unit representation:

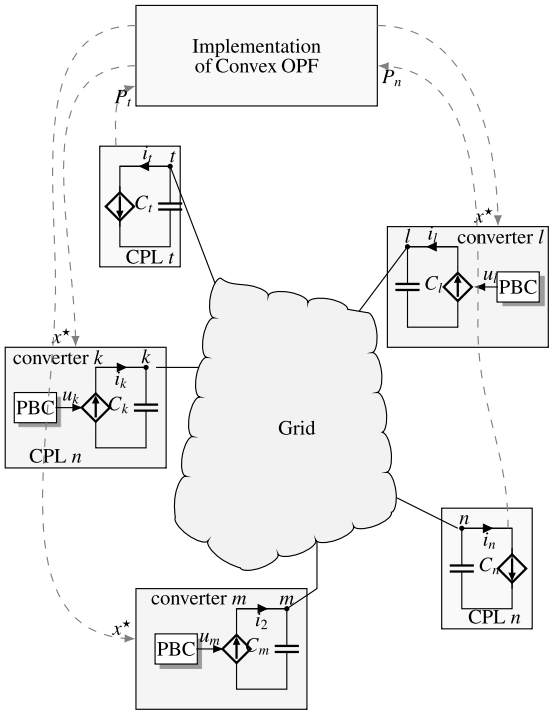

Fig. 5. Proposed hierarchical control scheme.

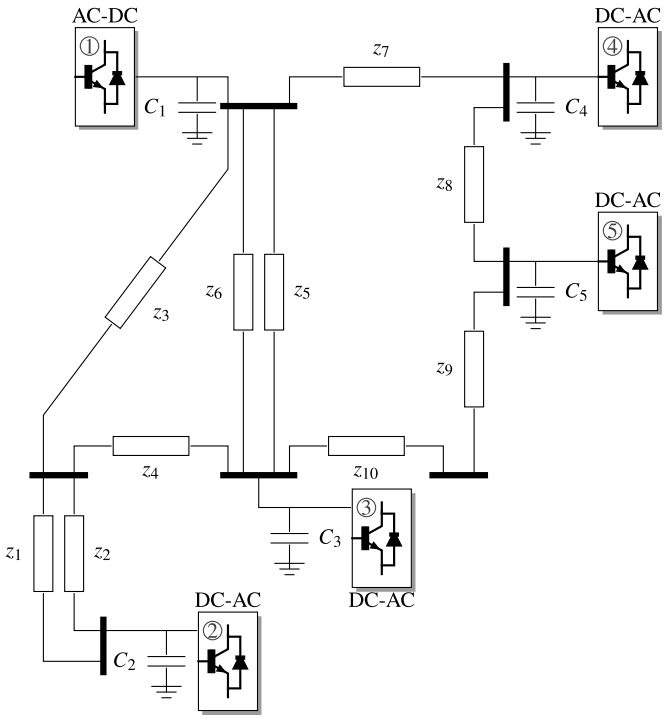

Fig. 6. Five multiterminal HVDC grid developed by the CIGRE B4 working group.

Table 1
Parametric information of the OHL and CBL.

Type	Res. (Ω/km)	Ind. (H/km)	Cap. (F/km)
OHL	0.0114	0.9356	0.0123
CBL	0.0095	2.1120	0.1906

Table 2
Information the HVDC lines.

Parameter	$Z_{1,2}$	Z_3	Z_4	$Z_{5,6}$	$Z_{7,8,10}$	Z_9
R_π (Ω)	3.42	5.70	2.28	4.56	1.90	2.85
L_π (H)	0.28	0.46	0.19	0.37	0.42	0.63
C_π (F)	1.85	3.08	1.23	2.46	19.06	28.60
Length (km)	300	500	200	400	200	300
Type	OHL	OHL	OHL	OHL	CBL	CBL

$$\mathscr{Y}_{\mathscr{H}} = \begin{bmatrix} 178.348 & -13.693 & -80.445 & -84.211 & 0 \\ -13.693 & 47.9247 & -34.232 & 0 & 0 \\ -80.445 & -34.232 & 148.361 & 0 & -33.684 \\ -84.211 & 0 & 0 & 168.421 & -84.211 \\ 0 & 0 & -33.684 & -84.211 & 117.895 \end{bmatrix}$$

We consider three load and generation steps as presented in Table 3.

6.1. OPF Solution

Next, we compare the effectiveness of the SDP approximation to solve the OPF problem with the nonlinear non-convex formulation (**Model 1**) in the general algebraic modeling system (GAMS), and the results are contrasted to the solution of **Model 2** provided by the CVX package from MATLAB.

Table 4 presents the solution of **Model 1** using the *Artelys Knitro 10.3.0* solver as well as the solution of **Model 2** provided by CVX. The SDP model's voltages present estimation errors lower than 1×10^{-3}% compared to the exact nonlinear model. These results confirm the convex model's accuracy and efficiency in terms of voltage calculation for the OPF problem in DC networks, as confirmed by different authors in [20–22].

The OPF model's solution using the convex proposed reformulation estimates a total power loss of 0.3615 p.u. with a tracking error lower than 2×10^{-4}% in comparison to the exact nonlinear non-convex OPF model. This validates its application, as reported in [20,21].

On the other hand, Table 5 shows the eigenvalues' behavior of the matrix of variables X used in the SDP model. This behavior also confirms that relaxing the rank of this matrix for obtaining a convex model is an adequate approximation for solving OPF problems since the values in Table 3 confirm that there exists a unique eigenvalue λ_5 that is different from zero. In contrast, the other eigenvalues are closer to zero, as supposed in (20).

An important fact in the proposed secondary/tertiary control stage is that it ensures that the solution to the OPF problem is optimal via SDP optimization. However, the generation values in PV sources can be different from the resource availability since the objective function is to minimize the total grid losses, which implies that the best solution corresponds to the set of powers that reduces the energy dissipation in the resistive effect of the grid. Table 6 presents the power injections in the PV node (node 5 in Fig. 6).

Note that in Table 6 it is possible to observe that in the first period, the amount of power injection in the PV sources is about 60.54 % of the total power availability, while for the rest of the periods, the PV generation is equal to the maximum power available. It is important to mention that if we fixed the generation in $\mathbf{T}_1$ as 2550 MW in the PV sources, then the total power losses in this period are about 8.8564 MW,

Table 3
Demand and generation information for three periods of time.

Node	T1 (MW)	T2 (MW)	T3 (MW)	Capacitance [μF]
1 Slack	—	—	—	75
2 CPT	850	1500	1200	275
3 CPT	1500	1400	2000	75
4 CPT	1850	2350	1500	4.5
5 PV	2550	500	1250	90

Table 4
Voltages obtaining by solving **Model 1** and **Model 2** with GAMS and CVX.

GAMS-KNITRO				
Period [s]	v_2 (p.u)	v_3 (p.u)	v_4 (p.u)	v_5 (p.u)
T1	0.96940387	0.98277874	0.98917412	1.00054847
T2	0.94812789	0.97359505	0.97524539	0.97910535
T3	0.95587639	0.97489993	0.98858684	0.99519122
		CVX-MATLAB		
Period [s]	v_2 (p.u)	v_3 (p.u)	v_4 (p.u)	v_5 (p.u)
T1	0.96936016	0.98271970	0.98906506	1.00034174
T2	0.94812784	0.97359505	0.97524544	0.97910548
T3	0.95592569	0.97496718	0.98870912	0.99543415

Table 5
Eigenvalues' behavior for the SDP convex approximation.

Period [s]	λ_1	λ_2	λ_3	λ_4	λ_5
T1	-3.221 × 10^{-09}	-2.463 × 10^{-09}	-2.223 × 10^{-09}	-9.685 × 10^{-10}	4.884
T2	-1.183 × 10^{-09}	-9.646 × 10^{-10}	-9.599 × 10^{-10}	-5.610 × 10^{-10}	4.757
T3	-6.196 × 10^{-10}	-4.972 × 10^{-10}	-4.464 × 10^{-10}	-2.598 × 10^{-12}	4.832

Table 6
Power injections in the PV node for all the demand load conditions.

Period	Nominal power (MW)	Injected power (MW)	p_{loss} (MW)
$\mathbf{T}_1$	2550	1543.7270	7.4222
$\mathbf{T}_2$	500	500	16.9014
$\mathbf{T}_3$	1250	1250	11.8075

which implies an increment of 1.4343 MW concerning the optimal solution. However, the solution that should be implemented will depend on the practices established by the power system operator bases on the market conditions regarding the usage of renewable energy resources instead of fossil sources.

6.2. Dynamic performance of the proposed PBC controls

We considered various numerical simulations using the MATLAB simpowersystems toolbox, including the transmission lines' inductive and capacitive effects. The control parameters were adjusted using multiple simulations to minimize the steady-state error. The values for $\mathscr{K}_p$ and $\mathscr{K}_I$ correspond to diagonal matrices with values between, which are varied from 0 to 20 for the proportional gains. At the same time, the integral gains are varied from 500 to 2500.

Fig. 7 shows the dynamic performance of the voltages in two network nodes. For this purpose, we select nodes 2 (load node) and 5 (generation node) since these present the most important voltages variations, as can be seen in Table 4.

The dynamic behavior obtained in Fig. 7 for the load and generation nodes allows observing that: (i) the usage of the proportional PBC control defined by Eq. (12) injects enough damping to the system in order to reduce the system oscillations and possible peaks caused by the reference changes; and (ii) the time of stabilization of the voltages in the system is highly dependent on the control gain since when the diagonal of $\mathscr{K}_p$ is an equation to time, the time to reach the reference is about 350 ms, while when the diagonal of the proportional gain is equal to 20, this time is reduced until 100 ms.

The PI action in the PBC control is analyzed in Fig. 8 which presents the performance of the voltage at node 5 (i.e., PV generation bus). The diagonal of the matrix $\mathscr{K}_p$ is assigned as 10, and the integral gains vary

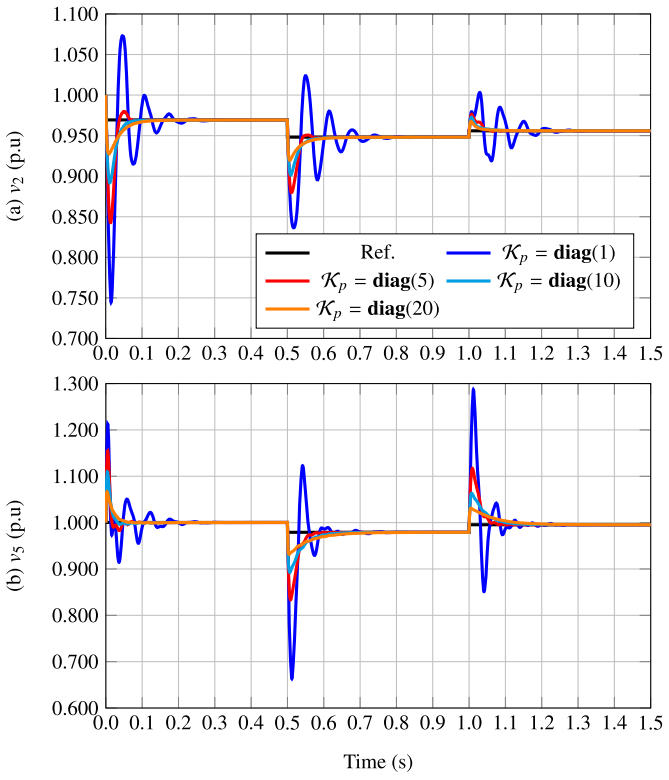

Fig. 7. Dynamic voltage performance a load and generation nodes: (a) voltage at node 2, and (b) voltage at node 5.

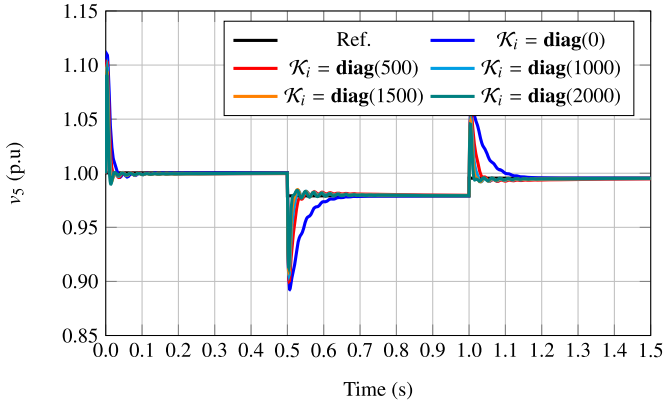

Fig. 8. Dynamic performance of the voltage in the PV node for different values of the integral gain.

from 0 to 2000 in steps of 500. The dynamic behavior of the voltage in this node shows that the integral gain in the PBC proposed control has two main effects: (i) it reduces the required time to reach the voltage reference, since, without integral gain, this time is about 150 ms when the proportional gain is set as 10; and less than 20 ms when is added the integral gain with a value of 2000, and (ii) the overpass of the voltages when the reference signal changes are lower when compared to the control with and without integral gains. This reduction is approximately 20 %.

6.3. Dynamic behavior the system in the presence of a short-circuit

The proposed passivity-based control guarantees the stable operation of the network when a large perturbation occurs inside of the network (e.g., short-circuit event). We simulate faults with different fault resistances (e.g., 10 Ω $\leq R_f \leq$ 50 Ω) at the node that connects lines 1 to 4 (see Fig. 6). Fig. 10 depicts the dynamic behavior of the voltage at node 2, which is the node with the largest load connected near the fault point. It is important to mention that in all the nodes with converters, the maximum variations of the control inputs, i.e., the powers are set as ± 4000 MW. Note that the duration of the fault is 100 ms, and the diagonal values of the proportional and integral control actions are set as 20 and 2000, respectively.

From Fig. 10, it possible to observe that: (i) for all the different resistances of fault, the proposed control allows stabilizing the system, e.g., for $R_f = 10$ Ω the stabilizing time is about 200 ms once the fault event is clarified, whereas $R_f = 50$ Ω the stabilizing time is less than 50 ms; (ii) the overpass in the voltage after clarifying the fault is dependent of the fault current, i.e., when $R_f = 10$ Ω the current fault in steady-state conditions is about 34.5 kA, which produce a voltage peak of 2.358 p.u, whereas for $R_f = 50$ Ω this current is about 7.7 kA and the maximum voltage peak is about 1.048 p.u; and (iii) the oscillations in the voltage after clarifying the fault are mainly caused by the effect of integral action due to the strong variations in the voltage reference and the measured signal; which can be attenuated with an adequate selection of the control gains.

6.4. Line disconnection and references updating

We simulate a possible topology variation in the network, where line Z_6 is disconnected in both extremes due to the non-correct operation of the protective devices. This new configuration of the network makes that the initial operative point of the network does not minimize the total grid losses, which implies that the references of the voltages provided to each power electronic converter must change to re-optimize the total power losses. To do this simulation, let us suppose that the grid initially operated with the conditions defined for T_1 in Table 3. To show that the system ensures the minimization of the power losses by updating the voltage references once the grid topology changes, we plot the total power generation in the slack source (see Fig. 10), i.e., node 1. Note that we assume that the information to solve the new optimization problem considering the new topology of the grid takes about 500 ms due to communication delays.

The behavior of the power generation at the slack node guaranteed that in steady-state conditions, the total power losses of the network are minimized by using the voltages' references provided by the secondary/tertiary control (i.e., solution of the OPF problem using the slack node). This implies that previous to the grid topology changes, the number of power losses of the grid is 7.4223 MW (see Fig. 10 before 2 s). During the period between 2 s and 2.5 s, the losses are not minimized; nevertheless, the proposed control allows stabilizing the system until the SDP model will provide the new references. When these references are reassigned to

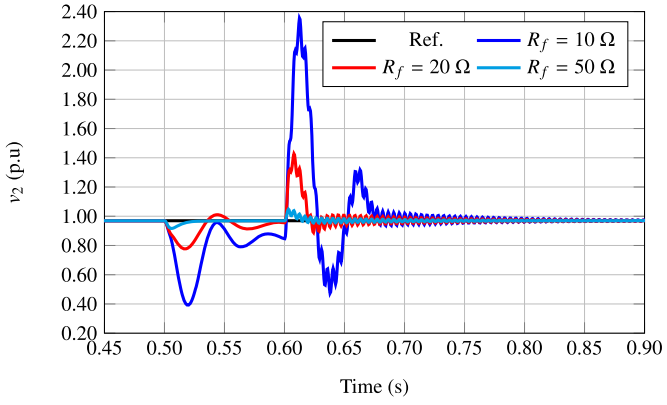

Fig. 9. Dynamic performance of the voltage at node 2 for different short-circuit events.

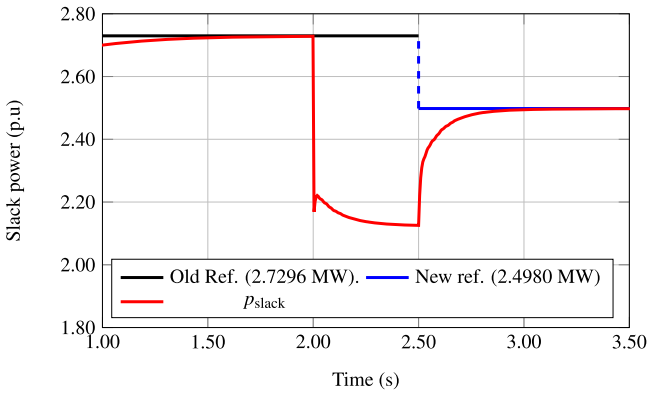

Fig. 10. Power generation at the slack node.

Data: Define DC grid topology and read the available power generation and consumptions.

$k = 1$;
for $t \geq t_0$ **do**
  if $k == 1$ **then**
    Solve the convex Model (17) ;
    Apply at each converter the control law in Eq. (11), (12), or (16);
    $k = 0$;
  else
    if *Any power generation has changed?* **then**
      $k = 1$;
    end
    if *Any CPT has changed?* **then**
      $k = 1$;
    end
  end
end

Algorithm 1. Proposed hierarchical control strategy for stabilizing DC networks.

the converters, the power generation in the slack node is optimal again, which implies that the power losses in steady-state conditions reach the desired value, i.e., 8.9856 MW.

7. Conclusion

This paper proposed a hybridization of a PBC and convex optimization via SDP to address MT-HVDC networks' hierarchical control with multiple DERs and CPTs. The primary control strategy was based on the PBC methods that guarantee global asymptotic stability using Lyapunov's theory in a closed-loop operation. Furthermore, the proposed PBC controls were based on proportional and PI actions that allow reaching the stabilization control objective by using only local measurements. This showed a clear advantage compared to PBC methods reported in the literature. Simultaneously, the set point of the PBC methods (the secondary/tertiary control stage) was defined with convex optimization, which relaxes the nonlinear non-convex model to guarantee uniqueness in the OPF solution. Different simulation results showed that the proposed hierarchical control strategy's was efficient and effective for stabilizing the DC network varying time load conditions.

Numerical simulations in the CIGRE five nodes multi-terminal HVDC test system demonstrated that the proposed hierarchical control maintains the system stable even if short-circuit events and grid configuration changes occur in the power system. Furthermore, when the configuration of the grid changes, the proposed SDP model can update all the voltage references in order to carry the test feeder to a new optimal operation point which minimizes the total grid losses.

As future works will be possible to develop the following research: (i) apply the model predictive control theory to replace the primary control stage to obtain a new control scheme that works with a unique optimization stage; (ii) replace the optimization stage based on the SDP model by a second-order cone programming equivalent to reduce the number of optimization variables, which reduces the computational charge of the proposed methodology; (iii) include in the mathematical modeling of the grid all the dynamics associated with the transmission lines.

CRediT authorship contribution statement

Oscar Danilo Montoya: Conceptualization, Methodology, Software, Validation, Formal analysis, Investigation, Resources, Data curation, Writing - original draft, Writing - review & editing, Visualization, Supervision, Project administration, Funding acquisition. **Walter Gil-González:** Conceptualization, Methodology, Software, Validation, Formal analysis, Investigation, Resources, Data curation, Writing - original draft, Writing - review & editing, Visualization. **Alejandro Garces:** Conceptualization, Methodology, Writing - review & editing. **Federico Serra:** Writing - original draft, Writing - review & editing, Visualization. **Jesus C. Hernández:** Writing - original draft, Writing - review & editing, Visualization.

Declaration of Competing Interest

The authors declare that they have no known competing financial interests or personal relationships that could have appeared to influence the work reported in this paper.

References

[1] O.D. Montoya, W. Gil-González, L. Grisales-Noreña, C. Orozco-Henao, F. Serra, Economic dispatch of BESS and renewable generators in DC microgrids using voltage-dependent load models, Energies 12 (23) (2019) 4494.
[2] J. Li, F. Liu, Z. Wang, S. Low, S. Mei, Optimal power flow in stand-alone DC microgrids, IEEE Trans. Power Syst. (2018) 1, https://doi.org/10.1109/TPWRS.2018.2801280.
[3] A. Garces, On convergence of newtons method in power flow study for DC microgrids, IEEE Trans. Power Syst. (2018) 1, https://doi.org/10.1109/TPWRS.2018.2820430.
[4] P. Magne, B. Nahid-Mobarakeh, S. Pierfederici, General active global stabilization of multiloads DC-Power networks, IEEE Trans. Power Electron. 27 (4) (2012) 1788–1798, https://doi.org/10.1109/TPEL.2011.2168426.
[5] A. Elnady, A. Adam, Decoupled state-Feedback based control scheme for the distributed generation system, Electric Power Components and Systems 46 (5) (2018) 494–510, https://doi.org/10.1080/15325008.2018.1453564.
[6] O.D. Montoya, W. Gil-González, A. Garces, Optimal power flow on DC microgrids: A Quadratic convex approximation, IEEE Trans. Circuits Syst. II Exp. Briefs (2018) 1, https://doi.org/10.1109/TCSII.2018.2871432.
[7] O.D. Montoya, W. Gil-González, L.F. Grisales-Noreña, Optimal power dispatch of DGs in DC power grids: a hybrid gauss-Seidel-Genetic-Algorithm methodology for solving the OPF problem, WSEAS Transactions on Power Systems 13 (33) (2018) 335–346.
[8] E. Benedito, D. del Puerto-Flores, A. Dória-Cerezo, J.M. Scherpen, Port-Hamiltonian based optimal power flow algorithm for multi-terminal DC networks, Control Eng. Pract. 83 (2019) 141–150, https://doi.org/10.1016/j.conengprac.2018.10.018.
[9] D. Murillo-Yarce, A. Garcés-Ruiz, A. Escobar-Mejía, Passivity-Based control for DC-Microgrids with constant power terminals in island mode operation, Revista Facultad de Ingeniería (86) (2018) 32–39.
[10] E. Benedito, D. del Puerto-Flores, A. Dória-Cerezo, J.M. Scherpen, Optimal power flow for resistive DC networks: a port-Hamiltonian approach, IFAC-PapersOnLine 50 (1) (2017) 25–30, https://doi.org/10.1016/j.ifacol.2017.08.005.
[11] C. De Persis, E.R. Weitenberg, F. Dörfler, A power consensus algorithm for DC microgrids, Automatica 89 (2018) 364–375, https://doi.org/10.1016/j.automatica.2017.12.026.
[12] M. Tucci, L. Meng, J.M. Guerrero, G. Ferrari-Trecate, Stable current sharing and voltage balancing in DC microgrids: a consensus-based secondary control layer, Automatica 95 (2018) 1–13, https://doi.org/10.1016/j.automatica.2018.04.017.
[13] M. Tucci, L. Meng, J.M. Guerrero, G. Ferrari-Trecate, Plug-and-play control and consensus algorithms for current sharing in DC microgrids, IFAC-PapersOnLine 50

(1) (2017) 12440–12445, https://doi.org/10.1016/j.ifacol.2017.08.1918.20th IFAC World Congress
[14] Z. Shuai, J. Fang, F. Ning, Z.J. Shen, Hierarchical structure and bus voltage control of DC microgrid, Renew. Sustain. Energy Rev. 82 (2018) 3670–3682, https://doi.org/10.1016/j.rser.2017.10.096.
[15] J. Lai, X. Lu, W. Yao, J. Wen, S. Cheng, Robust distributed cooperative control for DC mircogrids with time delays, noise disturbances, and switching topologies, J. Franklin Inst. 354 (18) (2017) 8312–8332, https://doi.org/10.1016/j.jfranklin.2017.10.025.
[16] C. Dong, F. Guo, H. Jia, Y. Xu, X. Li, P. Wang, DC Microgrid stability analysis considering time delay in the distributed control, Energy Procedia 142 (2017) 2126–2131, https://doi.org/10.1016/j.egypro.2017.12.616.Proceedings of the 9th International Conference on Applied Energy
[17] N. Vafamand, M.H. Khooban, T. Dragičević, F. Blaabjerg, Networked fuzzy predictive control of power buffers for dynamic stabilization of DC microgrids, IEEE Trans. Ind. Electron. 66 (2) (2019) 1356–1362, https://doi.org/10.1109/TIE.2018.2826485.
[18] M.A. Kardan, M.H. Asemani, A. Khayatian, N. Vafamand, M.H. Khooban, T. Dragičević, F. Blaabjerg, Improved stabilization of nonlinear DC microgrids: cubature kalman filter approach, IEEE Trans. Ind. Appl. 54 (5) (2018) 5104–5112, https://doi.org/10.1109/TIA.2018.2848959.
[19] L.F. Grisales-Noreña, O.D. Garzón-Rivera, J.A. Ocampo-Toro, C.A. Ramos-Paja, M. A. Rodriguez-Cabal, Metaheuristic optimization methods for optimal power flow analysis in DC distribution networks, Transactions on Energy Systems and Engineering Applications 1 (1) (2020) 13–31, https://doi.org/10.32397/tesea.vol1.n1.2.
[20] O.D. Montoya, Numerical approximation of the maximum power consumption in DC-MGs with CPLs via an SDP model, IEEE Trans. Circuits Syst. II Exp. Briefs 66 (4) (2018) 642–646, https://doi.org/10.1109/TCSII.2018.2866447.
[21] W. Gil-González, O.D. Montoya, E. Holguín, A. Garces, L.F. Grisales-Noreña, Economic dispatch of energy storage systems in dc microgrids employing a semidefinite programming model, J. Energy Storage 21 (2019) 1–8, https://doi.org/10.1016/j.est.2018.10.025.
[22] A. Garces, O.D. Montoya, R. Torres, Optimal power flow in multiterminal HVDC systems considering DC/DC converters. 2016 IEEE 25th International Symposium on Industrial Electronics (ISIE), 2016, pp. 1212–1217, https://doi.org/10.1109/ISIE.2016.7745067.
[23] O.D. Montoya, L. Grisales-Noreña, D. González-Montoya, C. Ramos-Paja, A. Garces, Linear power flow formulation for low-voltage DC power grids, Electr. Power Syst. Res. 163 (2018) 375–381, https://doi.org/10.1016/j.epsr.2018.07.003.
[24] J.W. Simpson-Porco, F. Dorfler, F. Bullo, On resistive networks of constant-Power devices, IEEE Trans. Circuits Syst. II Exp. Briefs 62 (8) (2015) 811–815, https://doi.org/10.1109/TCSII.2015.2433537.
[25] C. Gavriluta, I. Candela, C. Citro, A. Luna, P. Rodriguez, Design considerations for primary control in multi-terminal VSC-HVDC grids, Electr. Power Syst. Res. 122 (2015) 33–41, https://doi.org/10.1016/j.epsr.2014.12.020.
[26] A. Garces, Uniqueness of the power flow solutions in low voltage direct current grids, Electr. Power Syst. Res. 151 (Supplement C) (2017) 149–153, https://doi.org/10.1016/j.epsr.2017.05.031.
[27] R. Cisneros, F. Mancilla-David, R. Ortega, Passivity-Based control of a grid-Connected small-Scale windmill with limited control authority, IEEE J. Emerg. Sel. Top. Power Electron. 1 (4) (2013) 247–259, https://doi.org/10.1109/JESTPE.2013.2285376.
[28] S.P. Nageshrao, G.A.D. Lopes, D. Jeltsema, R. Babuska, Port-Hamiltonian systems in adaptive and learning control: A Survey, IEEE Trans. Autom. Control 61 (5) (2016) 1223–1238, https://doi.org/10.1109/TAC.2015.2458491.
[29] W. Gil-González, A. Garces, A. Escobar, Passivity-based control and stability analysis for hydro-turbine governing systems, Appl. Math. Modell. 68 (2019) 471–486, https://doi.org/10.1016/j.apm.2018.11.045.
[30] O.D. Montoya, W. Gil-González, F.M. Serra, PBC Approach for SMES devices in electric distribution networks, IEEE Trans. Circuits Syst. II Exp. Briefs (2018) 1–6, https://doi.org/10.1109/TCSII.2018.2805774.
[31] F.M. Serra, C.H.D. Angelo, IDA-PBC Controller design for grid connected front end converters under non-ideal grid conditions, Electr. Power Syst. Res. 142 (2017) 12–19, https://doi.org/10.1016/j.epsr.2016.08.041.
[32] A.M. Jubril, A.O. Adediji, O.A. Olaniyan, Solving the combined heat and power dispatch problem: A Semi-definite programming approach, Electric Power Components and Systems 40 (12) (2012) 1362–1376, https://doi.org/10.1080/15325008.2012.694972.
[33] A.M. Jubril, A.O. Adediji, Semi-definite programming approach to stochastic combined heat and power environmental/economic dispatch problem, Electric Power Components and Systems 43 (18) (2015) 2039–2049, https://doi.org/10.1080/15325008.2015.1075082.
[34] W. Gil-González, O.D. Montoya, E. Holguín, A. Garces, L.F. Grisales-Noreña, Economic dispatch of energy storage systems in dc microgrids employing a semidefinite programming model, Journal of Energy Storage 21 (2019) 1–8.